A Design Method for Synthesizing a Dual-Passband FSS for Wi-Fi Using Equivalent Circuit Model

Yuan Xu and Mang He

School of Information and Electronics
Beijing Institute of Technology, Beijing, 100081, China
hemang@bit.edu.cn

Abstract ─ In this letter, a dual-passband frequency selective surface (FSS) at Wi-Fi operation bands is presented. The proposed structure is implemented by two-dimensional periodic array of double square slots on single dielectric layer, which can be used to isolate the intensive care rooms of hospitals from insignificant signals, but supports Wi-Fi features, enabling doctors to acquire the patients' health condition at any time. The design procedure is based on the equivalent circuit method (ECM) combined with the genetic algorithm (GA) curve-fitting, which aims at providing the initial dimension parameters of FSS. Ultimately, the calculated results from the ECM are compared with the numerical results of the HFSS optimization, and the measured frequency response of the fabricated FSS covers all the Wi-Fi frequency bands, which verify the reliability of this design.

Index Terms ─ Equivalent circuit method, frequency selective surface, genetic algorithm, Wi-Fi.

I. INTRODUCTION

Nowadays, Wi-Fi has brought mobility and flexibility to our lives by different kinds of wireless devices. For example, the devices in Intensive Care Units (ICUs) of hospital use Wi-Fi to support the communication of the patients' health condition to doctors outside the rooms [1]. However, the distraction of other insignificant signals should be isolated from the rooms to minimize the impact on the precision equipment.

Frequency selective surfaces (FSSs) have been an important subject for their widespread applications as spatial filters for decades of years [2]. The feature of transmission at resonant frequency allows FSS to perform like a bandpass filter in Wi-Fi applications to improve transmission of RF/MW signals through shell [3-5]. Motivated by the ICUs' requirement, the bandpass FSS designed in this paper is applied as the shielding screen between ICUs and the outside world to isolate the rooms from the impact of insignificant signals, yet to allow Wi-Fi frequencies to pass through. According to the standard of IEEE 802.11n, the frequency band of the fourth generation Wi-Fi contains two parts: 2.4 GHz - 2.4835 GHz, and 5.15 GHz - 5.850 GHz. It is important to guarantee the transmission of electromagnetic (EM) wave at these two bands in the screen design.

Commonly, the design of FSS mainly relies on the full-wave numerical software [6-8], and the parametric sweep is an indispensable process. However, although the numerical simulations yield accurate frequency response for a given FSS structure, they cannot provide adequate information of how to start an FSS design and how to initialize the geometrical sizes of the design to fulfill the expected frequency response in a general form. In this letter, the equivalent circuit method is introduced to provide the initial design parameters of an FSS from the desired frequency response. For the dual-band design in Wi-Fi bands, we use the periodic elements of square slot (SS) and square loop (SL) [9], whose surface impedances in both the normal- and oblique-incidence situations [10-13] are studied in detail, to present band-pass and band-stop performances. In the synthesizing process [14, 15], equivalent circuit (EC) parameters and then the geometrical sizes of the structure can be obtained from a few typical *S*-parameter (S_{11}/S_{21}) samplings of the desired response curves via the genetic algorithm (GA) curve-fitting technique [16-18].

Ultimately, the dual-passband FSS designed by ECM, works well at Wi-Fi bands with the stability for different incident angles. Compared with the existing structure [1, 3-5, 19], this design has a simple structure and covers all the Wi-Fi operation frequency bands at normal and oblique incidence. For the sake of demonstration, a prototype of the FSS was fabricated and measured.

II. STRUCTURE DESCRIPTION AND OPERATING PRINCIPLES

A. Structure description

As mentioned in [2], the FSS composed of the SS elements is a bandpass filter. To obtain the two passbands for Wi-Fi application, the structure of double square slots can be chosen to construct the desired FSS. Figure 1 (a) shows the geometrical structure of this single-

Submitted On: March 21, 2019
Accepted On: May 12, 2019

layer FSS element. The metal part is printed on the top side of support dielectric medium whose thickness is d (the relative permittivity is ε_r, and the length of period element period is D). The length of the larger loop is l_1, and the width is w_1. The length of the smaller loop is l_2, and the width is w_2.

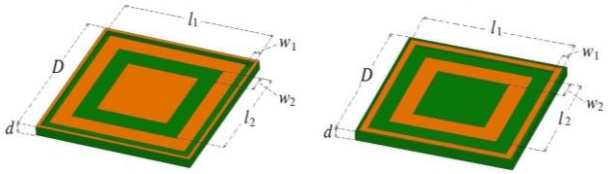

(a) (b)

Fig. 1. (a) The element of double square slots FSS (dual-passband), and (b) the element of double square loops FSS (dual-stopband). The structure in (b) is complementary to the structure in (a). The metal part is orange in color.

B. Design procedure

To determine the dimensions of the proposed structure, the design procedure contains:

Step 1. Obtain the equivalent circuit model of the FSS;

Step 2. Derive the impedance of metal layer;

Step 3. Build the transmission matrix based on the transmission line principle;

Step 4. Synthesize the EC parameters and then the geometrical sizes of the structure from a few typical S-parameter (S11/S21) samplings of the desired response curves via GA curve-fitting process;

Step 5. Optimize the FSS parameters based on the ECM data.

In step 1, it's difficult to judge whether the equivalent circuit of two square slots in Fig. 1 (a) are serial or parallel connected. However, the complementary structure of slots - double square loops (see Fig. 1 (b)) whose frequency response is dual stopband, has been studied in [20, 21], and its equivalent circuit is shown in Fig. 2, where the slots between loops present equivalent capacitance, and the strips represent the inductance. So, there are two serial LC resonators (L_1 - C_1 and L_2 - C_2) in the patch structure. Consequently, in this letter, we choose to pay attention to the square loops first, to simplify the equivalent circuit model. Later, using the Babinet's principle, it is easy to obtain the impedance of slots structure.

In step 2, as mentioned above, to obtain the impedance of the double square slots FSS layer, we should achieve the impedance of its complementary structure (SL). As shown in Fig. 2, the impedance of the patch FSS in different polarization can be depicted as:

$$Z_{SL}^{TE} = (j\omega L_1 + 1/\ j\omega C_1) \| (j\omega L_2 + 1/\ j\omega C_2) / \xi\,, \quad (1)$$

$$Z_{SL}^{TM} = (j\omega L_1 + 1/\ j\omega C_1) \| (j\omega L_2 + 1/\ j\omega C_2)\,, \quad (2)$$

where, $\xi = 1 - sin^2\theta / 2\varepsilon_{eff}$ is the influence factor of the incident angle θ [10]. Based on the equations in [10, 22], the circuit parameters in Fig. 2 can be derived as:

$$L_1 = \frac{\mu_0 l_1}{2\pi} \ln(1/\sin\frac{\pi w_1}{2D})\,, \quad (3)$$

$$C_1 = \varepsilon_0 \varepsilon_{eff} \frac{2l_1}{\pi} \ln[1/\sin\frac{\pi(D-l_1)}{2D}]\,, \quad (4)$$

$$L_2 = \frac{\mu_0 l_2}{2\pi} \ln(1/\sin\frac{\pi w_2}{2D})\,, \quad (5)$$

$$C_2 = \varepsilon_0 \varepsilon_{eff} \frac{l_2}{\pi} \ln[1/\sin\frac{\pi(l_1 - l_2 - 2w_1)/2}{2D}]\,, \quad (6)$$

the geometrical parameters are determined in Fig. 1, and ε_0 and μ_0 are the electromagnetic parameters of free space. The effective permittivity ε_{eff} of single layer FSS here is defined as:

$$\varepsilon_{eff} = \frac{\varepsilon_r + 1}{2} - \frac{\varepsilon_r - 1}{2} \exp[(-700d)^3]\,, \quad (7)$$

where, d and ε_r are the thickness and permittivity of the dielectric medium.

Then, applying the Babinet's principle:

$$Z_{SL}^{TE} Z_{SS}^{TM} = \frac{\eta_{eff}^2}{4}\,, \quad (8)$$

$$Z_{SL}^{TM} Z_{SS}^{TE} = \frac{\eta_{eff}^2}{4}\,, \quad (9)$$

where $\eta_{eff} = \sqrt{\mu_0 / (\varepsilon_0 \varepsilon_{eff})}$ is the effective wave impedance, we can obtain the impedance of double square slots $Z_{SS}^{TE,TM}$.

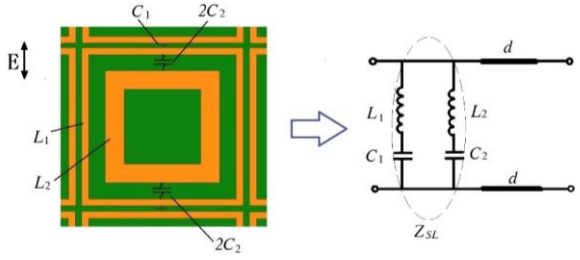

Fig. 2. The equivalent circuit of double square loops FSS.

In step 3, the medium below the metal patches can be regarded as a short transmission line in the circuit. So, the analytical transmission coefficients S_{21} for TE/TM polarization can be obtained from [23]:

$$S_{21} = \frac{2}{(A + B/Z_0^{TE,TM}) + (Z_0^{TE,TM} C + D)}\,, \quad (10)$$

$$Z_0^{TE} = Z_0 / \cos(\theta), Z_0^{TM} = Z_0 \cos(\theta)\,, \quad (11)$$

where, Z_0 is the intrinsic wave impedance in free space. According to the equivalent circuit shown in Fig. 2, the ABCD matrix can be written as the product of two cascade matrices:

$$\begin{bmatrix} A & B \\ C & D \end{bmatrix} = \begin{bmatrix} 1 & 0 \\ 1/Z_{SS}^{TE,TM} & 1 \end{bmatrix} \begin{bmatrix} \cosh(j\theta_1) & Z_1 \sinh(j\theta_1) \\ Y_1 \sinh(j\theta_1) & \cosh(j\theta_1) \end{bmatrix}, \quad (12)$$

where the parameters are as follows,

$$Z_1^{TE} = \omega\mu_0 / \beta_1, Z_1^{TM} = \beta_1 / \omega\varepsilon_0\varepsilon_r,$$

$$Y_1 = 1/Z_1, \theta_1 = \beta_1 d,$$

$$\beta_1 = \sqrt{k_1^2 - k_t^2}, k_t = k_0 \sin(\theta), k_1 = k_0\sqrt{\varepsilon_r}, \quad (13)$$

where k_t is the transverse vector, k_1 is the propagation constant in the substrate, and k_0 is the wave number in free space.

In step 4, we determine the dielectric substrate has a thickness of 1.27 mm and the relative permittivity of 2.2. To synthesize the unknown geometrical parameters: l_1, w_1, l_2, w_2, and D, we apply the GA curve-fitting method on the samplings from the desired S_{21} curve. Here, several sampling frequencies and the corresponding values of $|S_{21}|$ are listed in Table 1, which manifest the main property of the dual passbands. In this method, to ensure the good transmission properties of the FSS in different incident angles and different polarizations, we introduce different weighting factors to the adaptive function:

$$fun = \sum_{r=1}^{2}\sum_{m=1}^{M}\sum_{n=1}^{N} W_n \left\{ W^{TE,TM} \left[\left| S_{21}^{TE,TM} \right|(m,n) - \left| S_{21}^{0} \right|(m) \right] \right\}, \quad (14)$$

where, r indicates the TE and TM polarization, m indicates the number of frequency points, and n indicates the number of angle points. $W^{TE,TM}$ is the weighting factor of TE/TM polarization, and W_n is the weighting factor of different incident angles. $\left|S_{21}^{TE,TM}\right|(m,n)$ is the magnitude of transmission coefficients at different frequencies and angles, which has been derived in step. 3, and $\left|S_{21}^{0}\right|(m)$ is the sampling points from the desired $|S_{21}|$ curve at different frequencies (in Table 1).

Table 1: Samples from the desired frequency response of $|S_{21}|$

Sampling Frequencies (GHz)	1.0	2.4	2.5	4.0	5.1
$\left\|S_{21}^{0}\right\|$ **(dB)**	-5.0	-0.5	-0.5	-15	-0.5
Sampling Frequencies (GHz)	5.3	5.5	5.7	5.9	
$\left\|S_{21}^{0}\right\|$ **(dB)**	0	0	0	-0.5	

In this design, we define: $W^{TE} = W^{TM} = 1$ (ensure the property for both TE and TM polarization), W_n = 1 ($\theta \le 45^\circ$) and W_n = 0.1 ($\theta > 45^\circ$) (ensure the property of oblique incidence θ = 0~45°). In the GA algorithm, FSS structural parameters are chosen as the parameters to be optimized, and seaching ranges are set to be: $15\ mm \le l_2 < l_1 < D \le 30\ mm, 0.1\ mm \le w_{1,2} \le 3\ mm$. Also the stopping criteria of GA is defined [24, 25]: the population size is 100, the number of max generations is 100, the number of stall generations is 50, the crossover fraction is 0.75, and the function tolerance is 1e-6. Using the GA optimization to minimize the adaptive function (14), the optimal unknown geometrical parameters can be obtained (see Table 2).

Table 2: Geometrical parameters calculated by the ECM and HFSS

	l_1 (mm)	w_1 (mm)	l_2 (mm)	w_2 (mm)	D (mm)
Optimal Values by ECM and GA	23.5	1.5	16.6	2.3	24.6
Optimal Values by HFSS' Parameter-Sweep	24.0	1.0	17.0	2.8	25.0

Then in step 5, the ECM data achieved from step 4 are used as the initial values in the parameter-sweep process in the ANSYS HFSS for fine tuning. The optimization results are compared with the ECM data in Table 2. It can be seen that the ECM data are close to the optimized structure dimensions, which will save lots of time for starting an FSS design. In addition, the effect of different dimension parameters can be easily achieved from the ECM equations, which offers many conveniences to the HFSS optimization. Based on this principle, it can be obtained that increasing the parameter w_2 properly will achieve the wide band in 5.15 GHz - 5.850 GHz.

III. SIMULATION AND EXPERIMENTAL VERIFICATION

A. ECM results and simulated results

Here, the optimization range of incident angle is 0°~45° as defined in step 4. Based on the analysis in Section II, the computed transmission coefficient $|S_{21}|$ (θ = 0° and 45°) with the structure sizes obtained by ECM is plotted in Fig. 3 (a), compared with the sampling points in Table 1. It's seen that the resonant frequencies of the response are close to the desired sampling points, which means the results of ECM almost presents the expected dual bands response.

The simulated $|S_{21}|$ (θ = 0° and 45°) from HFSS with the optimization sizes in Table 2 from step 5 is shown in Fig. 3 (b), as well as the results of TE- and TM-polarization. The results in Fig. 3 (b) present that the FSS we design can guarantee the transmission of EM wave (transmission efficiency is more than 80%) even the incident angle is up to 45° in both Wi-Fi bands: 2.4 GHz - 2.4835 GHz, and 5.15 GHz - 5.850 GHz. In addition,

the optimal values by HFSS are in close proximity to the calculated sizes given by the proposed ECM. The good simulated results indicate this design of FSS is qualified to the Wi-Fi application.

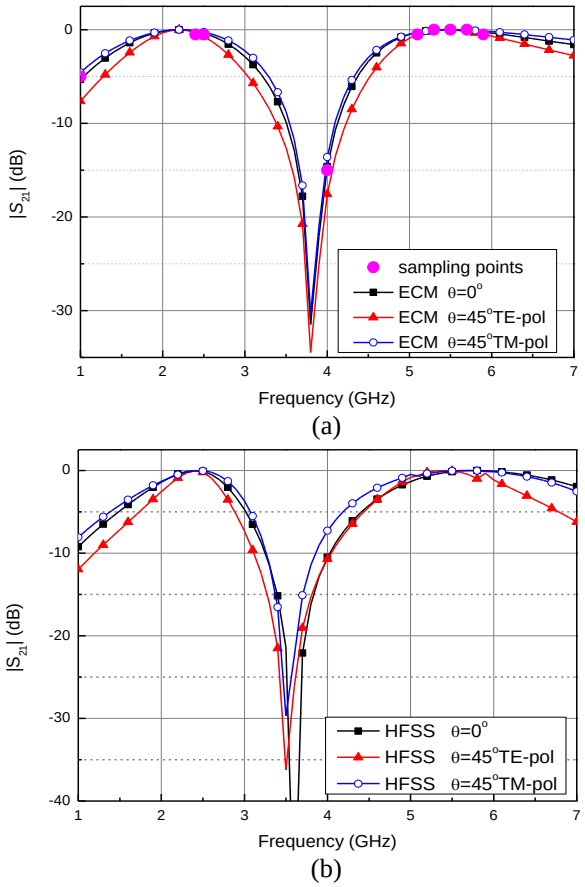

Fig. 3. (a) $|S_{21}|$ of FSS with the synthesized sizes by ECM calculation, and (b) $|S_{21}|$ of the FSS with optimal sizes fine-tuned by HFSS simulations.

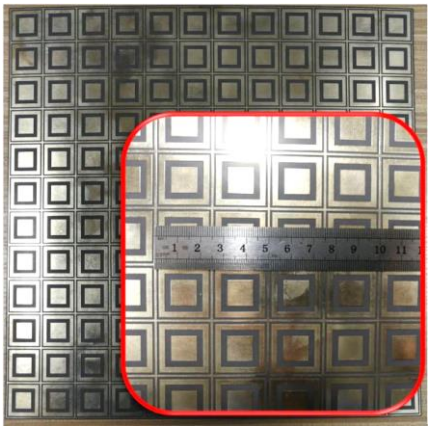

Fig. 4. The top view photo of the fabricated FSS.

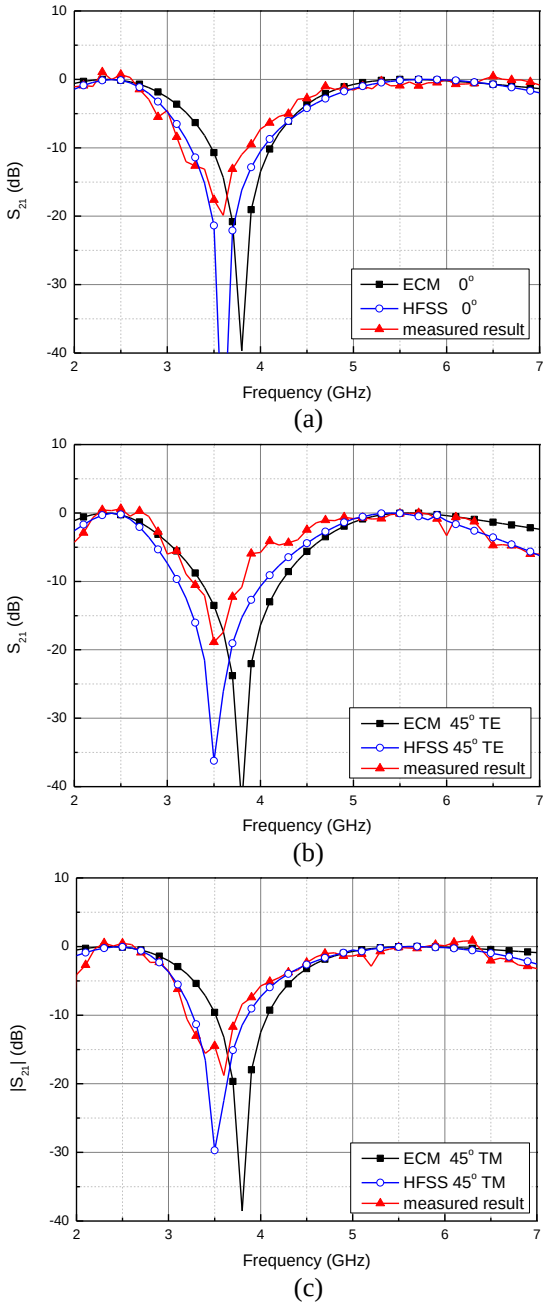

Fig. 5. Measured results compared with the calculated results from ECM and HFSS: (a) $|S_{21}|$ of normal incidence, (b) $|S_{21}|$ of oblique incidence θ = 45° for TE-polarization, and (c) $|S_{21}|$ of oblique incidence θ = 45° for TM-polarization.

B. Experimental verification

To validate the performance of the proposed FSS, a proto-type is fabricated and measured. The prototype is fabricated on Arlon DiClad 880 dielectric substrate (see Fig. 4), of which the permittivity is 2.2, loss tangent is

0.0009, and the thickness is 1.27 mm. The dimensions of FSS elements follow the final optimized data by HFSS in Table 2. The physical dimensions of the FSS arrays are 30.00 cm × 30.00 cm, which means the number of elements is 12 × 12. Then, the measurement was performed with the setup consisting of two broadband horn antennas for transmitting and receiving EM wave, respectively. During the measurement of the transmission coefficient of the FSS, we first need to measure the $|S_{21}|$ between the horn antennas without the FSS as the calibration data, and then we measure again the $|S_{21}|$ between the two horns when the FSS under test is present. Finally, the $|S_{21}|$ of the FSS itself is obtained by normalizing the $|S_{21}|$ measured in the second time to the calibration data.

Limited by the experiment conditions, the measurement starts from the frequency of 2 GHz to 7 GHz. The measured results of $|S_{21}|$ are compared with the numerical results by ECM and HFSS using the same structure parameters in Fig. 5, when the angle and polarization of incidence varies. As can be seen, the measured results agree well with the simulated ones from HFSS, indicating two passbands: 2.4 GHz - 2.4835 GHz, and 5.15 GHz - 5.850 GHz, with $|S_{21}| \geq$ -1.5 dB, and a stopband at 3.6 GHz, with $|S_{21}| \leq$ -15 dB. In addition, the FSS works stably when the angle of incidence increases up to 45°. At the same time, it is found in Fig. 5 that the measured frequency responses have small ripples over the frequency range, which is possibly caused by truncation and assembly errors between the transmit and receive antennas. As well, ECM results show similar properties except for a slight difference, which is caused by the accuracy of the equivalent circuit formulations is less than the full-wave simulation, and we'll improve it in our future work. Nevertheless, the fabricated prototype meets the desired requirements quite well, which indicates that the proposed design procedure using ECM is feasible and effective.

IV. CONCLUSION

This letter proposes a dual-passband single-layer FSS based on the classic structure of double square slots used in the ICUs to allow the Wi-Fi signals to pass through, and to isolate the insignificant signals. The design procedure applies the method of equivalent circuit and genetic algorithm to determine the FSS's geometrical parameters. To reduce the difficulty in analyzing slots structure, we put forward the approach of introducing complementary structure and obtaining the impedance of slots by Babinet's principle afterwards. The synthesized geometrical sizes given by the proposed ECM are in close proximity to the optimized values by HFSS, which means the ECM is qualified to start an FSS design. This design method provides a convenient way to realize the dimension estimation of the desired FSS, which will save much time in the design process. Besides, the measured results of fabrication cover all the Wi-Fi working bands both in normal- and oblique-incidence situation, which validate the reliability of this design method.

REFERENCES

[1] S. I. Sohail, "Wi-Fi transmission and multi-band shielding using single-layer frequency selective surface," *2016 IEEE International Symposium on Antennas and Propagation (APSURSI)*, Fajardo, pp. 963-964, 2016.

[2] B. A. Munk, *Frequency Selective Surface: Theory and Design*. New York: Wiley-Interscience, pp. 1-22, 2000.

[3] D. Hamzaoui, T. P. Vuong, F. Djahli, and G. I. Kiani, "Novel compact dual-band artificial magnetic conductors for Wi-Fi applications," *The 8th European Conference on Antennas and Propagation (EuCAP 2014)*, The Hague, pp. 2397-2400, 2014.

[4] I. Ullah, X. Zhao, D. Habibi, and G. Kiani, "Transmission improvement of UMTS and Wi-Fi signals through energy saving glass using FSS," *WAMICON 2011 Conference Proceedings*, Clear-water Beach, FL, pp. 1-5, 2011.

[5] D. Ferreira, I. Cuinas, and R. F. S. Caldeirinha, "Dual-band single-layer quarter ring frequency selective surface for Wi-Fi applications," *IET Microw. Antennas Propag*., vol. 10, pp. 435-441, 2016.

[6] X. Sheng, J. Fan, N. Liu, and C. Zhang, "A miniaturized dual-band FSS with controllable frequency resonances," *IEEE Microwave and Wireless Components Lett.*, vol. 27, no. 10, pp. 915-917, Oct. 2017.

[7] S. Ünaldı, S. Çimen, G. Çakır, and U. E. Ayten, "A novel dual-band ultrathin FSS with closely settled frequency response," *IEEE Antennas and Wireless Propag. Lett.*, vol. 16, pp. 1381-1384, 2017.

[8] M. Z. Joozdani and M. K. Amirhosseini, "Equivalent circuit model for the frequency-selective surface embedded in a layer with constant conductivity," *IEEE Trans. Antennas and Propag.*, vol. 65, no. 2, pp. 705-712, Feb. 2017.

[9] D. Ferreira, R. F. S. Caldeirinha, I. Cuiñas, and T. R. Fernandes, "Square loop and slot frequency selective surfaces study for equivalent circuit model optimization," *IEEE Trans. Antennas and Propag.*, vol. 63, no. 9, pp. 3947-3955, Sept. 2015.

[10] O. Luukkonen and C. Simovski, "Simple and accurate analytical model of planar grids and high-impedance surfaces comprising metal strips or patches," *IEEE Trans. Antennas and Propag.*, vol. 56, no. 6, pp. 1624-1632, June 2008.

[11] R. J. Langley and E. A. Parker, "Equivalent circuit model for arrays of square loops," in *Electronics Letters*, vol. 18, no. 7, pp. 294-296, 1 Apr. 1982.

[12] C. K. Lee and R. J. Langley, "Equivalent-circuit models for frequency-selective surfaces at oblique angles of incidence," in *IEE Proceedings H - Microwaves, Antennas and Propagation*, vol. 132, no. 6, pp. 395-399, Oct. 1985.

[13] G. H. Sung, K. W. Sowerby, M. J. Neve, and A. G. Williamson, "A frequency-selective wall for interference reduction in wireless indoor environments," in *IEEE Antennas and Propagation Magazine*, vol. 48, no. 5, pp. 29-37, Oct. 2006.

[14] N. Liu, X. Sheng, C. Zhang, and D. Guo, "Design of frequency selective surface structure with high angular stability for radome application," *IEEE Antennas Wireless Propag. Lett.*, vol. 17, no. 1, pp. 138-141, Jan. 2018.

[15] N. Liu, X. Sheng, C. Zhang, J. Fan, and D. Guo, "A design method for synthesizing wideband band-stop FSS via its equivalent circuit model," *IEEE Antennas Wireless Propag. Lett.*, vol. 16, pp. 2721-2725, 2017.

[16] G. Manara, A. Monorchio, and R. Mittra, "Frequency selective surface design based on genetic algorithm," *Electronics Letters*, vol. 35, pp. 1400-1401, 1999.

[17] E. F. Kent, B. Doken, and M. Kartel, "A new equivalent circuit based FSS design method by using genetic algorithm," *International Conference on Engineering Optimization*, pp. 1-4, 2010.

[18] Z. Li, P. Y. Papalambros, and J. L. Volakis, "Frequency selective surface design by integrating optimization algorithms with fast full wave numerical methods," *IEE Proc. Microw. Antennas Propag.*, vol. 149, no. 3, pp. 175-180, 2002.

[19] X. Xiong, W. Hong, Z. Zhao, L. Deng, and S. Li, "Wi-Fi band-stop FSS for increased privacy protection in smart building," *2015 IEEE 6th International Symposium on Microwave, Antenna, Propagation, and EMC Technologies (MAPE)*, Shanghai, pp. 826-828, 2015.

[20] R. J. Langley and E. A. Parker, "Double-square frequency-selective surfaces and their equivalent circuit," *Electronics Letters*, vol. 19, no. 17, pp. 675-677, 18 Aug. 1983.

[21] M. Yan, J. Wang, and H. Ma, "A tri-band, highly selective, bandpass FSS using cascaded multilayer loop arrays," *IEEE Trans. Antennas and Propag.*, vol. 64, no. 5, pp. 2046-2049, May 2016.

[22] F. Costa, A. Monorchio, and G. Manara, "An overview of equivalent circuit modeling techniques of frequency selective surfaces and metasurfaces," *Applied Computational Electromagnetics Society Journal*, no. 29, pp. 960, 2014.

[23] H. Li, Q. Cao, C. Yang, and Y. Wang, "Design and analysis of a frequency selective radome (FSR) with wideband absorbing properties," *2016 IEEE International Workshop on Electromagnetics: Applications and Student Innovation Competition (iWEM)*, Nanjing, pp. 1-3, 2016.

[24] A. J. Chipperfield and P. J. Fleming, "The MATLAB genetic algorithm toolbox," *IEE Colloquium on Applied Control Techniques Using MATLAB*, London, UK, pp. 10/1-10/4, 1995.

[25] Y. Rahmat-Samii, *Electromagnetic Optimization by Genetic Algorithms*. Wiley Series in Microwave and Optical Engineering, 1999.